Statistical Reports

Ecology, 100(2), 2019, e02580

Non-circular home ranges and the estimation of population density

M. G. Efford[1]

Department of Mathematics and Statistics, University of Otago, P.O. Box 56, Dunedin 9054 New Zealand

Citation: Efford, M. G. 2019. Non-circular home ranges and the estimation of population density. Ecology 100(2):e02580. 10.1002/ecy.2580

Abstract. Spatially explicit capture–recapture (SECR) models have emerged as one solution to the problem of estimating the population density of mobile and cryptic animals. Spatial models embody assumptions regarding the spatial distribution of individuals and the spatial detection process. The detection process is modeled in SECR as a radial decline in detection probability with distance from the activity center of each individual. This would seem to require that home ranges are circular. The robustness of SECR when home ranges are *not* circular has been the subject of conflicting statements. Ivan et al. previously compared the SECR density estimator to a telemetry-scaled non-spatial estimator. I suggest that the apparent non-robustness of SECR in their study was a simulation artefact. New simulations of elliptical home ranges establish that the SECR density estimator is largely robust to non-circularity when detectors are spread in two dimensions, but may be very biased if the detector array is linear and home ranges align with the array. Transformation to isotropy reduces bias from designs of intermediate dimension, such as hollow square arrays. Possible alignment of home ranges should be considered when designing detector arrays.

Key words: anisotropic detection function; density estimation; home range; non-circularity; radiotelemetry; spatially explicit capture–recapture; study design; telemetry-scaled non-spatial estimator.

INTRODUCTION

Population density is a parameter of central importance in ecology, but one that has proved hard to measure for species that are mobile and cryptic. When captures of mobile animals accumulate over time, as in trapping studies, it is hard to define the extent of the population from which they are drawn. It is presumably greater than a polygon drawn around the outermost traps, but how much greater? Spatially explicit capture–recapture (SECR) models avoid this question by estimating density directly from spatial capture–recapture data (Efford 2004, Borchers and Efford 2008, Royle and Young 2008, Efford et al. 2009, Royle et al. 2014). Density is a property of the spatial distribution of individuals; each individual is represented in SECR by a unique stationary point (activity center) that is central to the home range in some sense. SECR models combine a spatial point process for activity centers with a spatial detection model, such as a monotonic decline in detection probability with distance from each activity center. The point process is naturally parameterized in terms of its intensity: a fitted SECR model estimates a density surface, and the expected number of activity centers within any region may be inferred post hoc from the volume under that surface (Efford and Fewster 2013). Alternatively, the model may be parameterized in terms of the number of activity centers in an arbitrary region (Royle et al. 2014).

SECR models estimate density from the location of detections without direct information on animal movement. When that information is available (from radiotelemetry, for example) there exists an alternative estimation strategy: a non-spatial estimate of population size may be scaled to obtain a rigorous and unbiased estimate of population density (Boutin 1984, White and Shenk 2001, Grant and Doherty 2007, Ivan et al. 2013*a*). The appropriate scaling factor is the average proportion of each individual's activity that lies within the designated study area; its units were conveniently labeled "animal equivalents" by Boutin (1984). The average over individuals of the fraction of telemetry records in the designated area provides an estimate of the scaling factor. The ad hoc nature of these density estimators has been mildly criticized (Royle et al. 2013), but statistical inelegance might be a small price to pay if the estimators have superior statistical properties (bias and precision).

Manuscript received 25 September 2018; revised 24 October 2018; accepted 6 November 2018. Corresponding Editor: Evan G. Cooch.

[1] E-mail: murray.efford@otago.ac.nz

The standard detection model in SECR (a monotonic decline with radial distance from the activity center) follows intuitively if home ranges are circular. A suitable model for the radial decline may be selected from among several candidates, such as half-normal or negative exponential. However, home ranges are almost never circular, and the assumption of circularity has been a recurring worry for users of SECR. The study of Ivan et al. (2013*b*; henceforth IWS) reinforced these concerns: simulations with a square trapping grid appeared to show that the SECR density estimator was biased when home ranges were not circular, while the telemetry-scaled non-spatial estimator (TELEM) was unaffected. SECR estimates also appeared to be less precise than TELEM estimates in their simulations.

Other authors have taken a more optimistic stance on the robustness of SECR estimators to non-circular home ranges. Efford (2004) predicted that non-circularity would reduce precision without greatly affecting bias. Borchers and Efford (2008) asserted that circular symmetry of the detection function “could just reflect our ignorance of the orientation of possibly asymmetric home ranges,” implying that estimates would be unaffected by range asymmetry.

In this report, I hope to reconcile conflicting perceptions of the robustness of SECR to non-circularity. Simulations are used to assess the robustness of SECR with randomly oriented elliptical home ranges of varying eccentricity, with results that differ from those of IWS. I suggest that the apparent non-robustness of SECR in the simulations of IWS was an artefact, and that the apparent difference in precision between SECR and TELEM in their simulations was a consequence of subtly differing benchmarks for “true” density; as a better basis for comparison, SECR may be used with telemetry data to estimate the “realized” spatial population on an arbitrarily small area. To test these ideas, I repeated the simulations of IWS, both with and without adjustments to remove the simulation artefacts.

Although SECR was robust to non-circularity per se in the preceding simulations, these represented only a subset of the possible configurations. Further simulations were undertaken to document the performance of the SECR density estimator when elongated ranges were oriented variously with respect to detector arrays of differing geometry. These show a potential for extreme bias. The bias may sometimes be reduced by transforming space so that aligned elliptical home ranges become circular (the anisotropic detection functions of Murphy et al. [2016]). I apply the anisotropic estimator to simulated data and identify conditions under which it is likely to be useful.

Simulated Performance of SECR With Randomly Oriented Elliptical Data

I describe simulations to assess the performance of the SECR density estimator for a bivariate normal model of animal activity in which the contours of equal probability density are ellipses (Jennrich and Turner 1969). Throughout this paper I use “home range” to mean the distribution of an individual’s activity, and assume that the hazard of detection is directly proportional to that distribution.

Three detector geometries are considered: a 10 × 10 square array (as simulated by IWS), a line of 36 detectors arranged in a 10 × 10 hollow square, and a straight line of 36 detectors. A square detector array samples movements in all four cardinal directions and in many intermediate directions. In contrast, recaptures on a linear array are constrained to lie along the axis of the array, and the spatial scale of detection in two dimensions may not be estimated reliably when home ranges are elongated and oriented consistently with respect to the detector array.

Home-range elongation is measured here by the aspect ratio of the ellipse (ratio of the lengths of the major and minor axes). The aspect ratio was varied between 1 and 4, and ellipses were initially oriented independently at random (Fig. 1a). The bivariate normal (BVN) scale parameters for aspect ratio a were $\sigma_x = 0.5\,s/\sqrt{a}$ and $\sigma_y = 0.5\,s\sqrt{a}$, where s was the detector spacing.

Home ranges were placed at a density of $0.25\ s^{-2}$ at uniform random centers across a square arena that extended $4s$ beyond the detectors. Detections were simulated over five sampling occasions, and assumed independence among detectors (i.e. the binary “proximity” detector type of Efford et al. [2009]). A circular half-normal detection function on the hazard scale was fitted to each simulated dataset by maximizing the conditional likelihood, and density was estimated as a derived parameter (Borchers and Efford 2008, Efford 2018). Estimator performance was summarized by the relative bias and mean relative standard error, estimated from 500 replicates, using the fixed density over the entire arena as the reference density. Simulations were performed in the R package secrBVN described in Appendix S1.

For a square grid, the simulations gave little support for the notion that the bias of density estimates from a mis-specified (circular) model depended on the aspect ratio of elliptical home ranges (Fig. 2). The estimated bias of −0.9% for the most elongated BVN home ranges (aspect ratio 4.0) was small compared with the mean relative standard error, and that varied little (7.7% for aspect ratio 1.0; 7.6% for aspect ratio 4.0). Results from square detector arrays under other scenarios for density and number of detectors produced similar results, and heterogeneity of aspect ratio did not introduce bias (Appendix S2). However, increasing elongation led to substantial bias when detectors were arranged in a straight line or hollow square (Fig. 2). This novel result is explored with further simulations in a later section.

Simulations of Ivan et al. (2013*b*)

The simulations of IWS with a square trapping grid indicated significant median bias of the SECR density estimator when home ranges were elliptical, which conflicts with the results in the preceding section. To

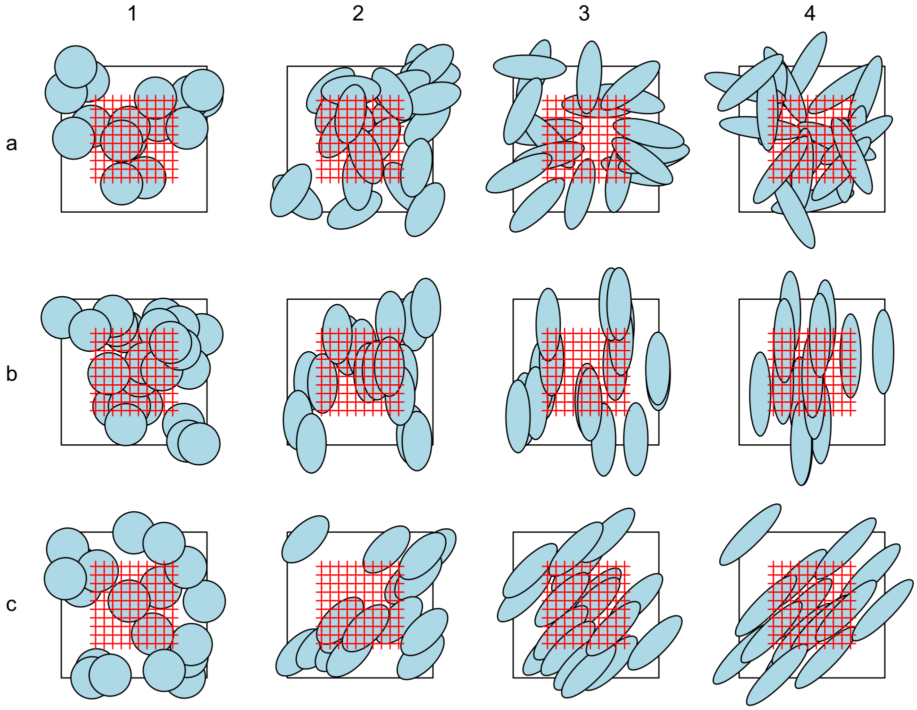

FIG. 1. Simulated elliptical home ranges of varying aspect ratio (1–4; columns) and orientation (rows) sampled with a square grid of detectors (red crosses). (a) Independent and random orientation, (b) aligned to grid, and (c) oblique to grid. Ellipses represent an arbitrary probability contour for a bivariate normal distribution of activity.

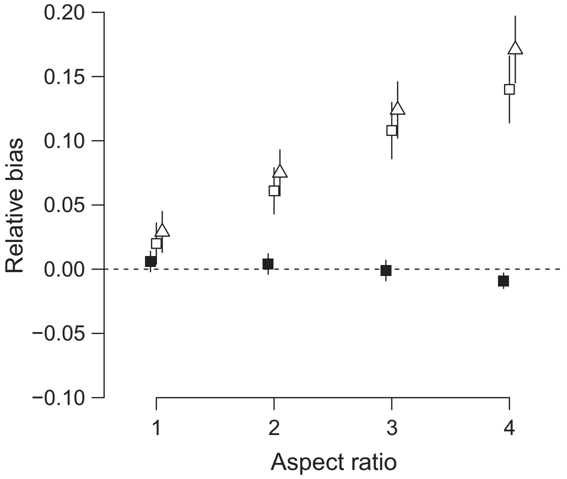

FIG. 2. Relative bias of simulated spatially explicit capture–recapture (SECR) density estimates when randomly aligned elliptical home ranges are sampled with three detector geometries, as a function of elongation (aspect ratio of ellipse). Solid squares, 10 × 10 grid; open squares, 10 × 10 hollow grid (36 detectors); open triangles, line (36 detectors). There were 500 simulations. Error bars show 95% confidence intervals.

investigate this discrepancy, I first reproduced their results in R (R Core Team 2018), with help from J. Ivan (*personal communication*; Appendix S1). I focus on a particular scenario in which 20 home ranges were placed in a square arena of 256 cells, with 100 cells in a central square designated as "traps"; each cell has sides of length *s*. Two types of home range were modelled, either (1) a bivariate normal distribution of activity (BVN) or (2) a set of 16 contiguous grid cells (CELLS). BVN home ranges could be circular ($\sigma_X = \sigma_Y = 0.921s$) or elliptical ($\sigma_X = 0.4s, \sigma_Y = 1.8s$; J. Ivan, *personal communication*). CELLS home ranges could be square (4 × 4), rectangular (2 × 8), or irregular (16 cells grown by random accretion from an initial cell); cell-specific activity was assigned from a uniform random distribution.

Home ranges were placed in the arena according to rules that depended on their shape. The lower left cell of square or rectangular home ranges was centered on a cell chosen at random from the 169 cells in the lower left of the arena. The initial cell of irregular home ranges was located likewise. The centroids of BVN home ranges were placed at random in a region bounded by the centroids of the outermost cells of the arena (not the arena boundary itself).

Other simulation details followed IWS. Telemetry data (the binomial proportion of activity inside the trapping area) were simulated for 75% of trapped animals, and predicted for the remainder by logistic regression from the location of captures (Ivan et al. 2013*a*).

Telemetry-scaled non-spatial estimator and SECR density estimates were computed and summarized as described by IWS. Fig. 3a–e matches their Fig. 3 for the key comparison between TELEM and SECR (curves for other estimators are omitted because they are of historical interest only). Median bias was apparent for

Statistical Reports

elongated (elliptical or rectangular) home ranges and for irregular home ranges (Fig. 3). The bias was relatively small (≈ −8%) for the elliptical ranges and large (≈ −20%) for both the rectangular and irregular ranges. We seek to explain these biases.

Consequences of placement rules

The shape-specific placement rules result in differing densities in the core area (the trap cells), and shape-specific low- or zero-density areas at the edge of the arena (Appendix S3: Fig. S2). I suggest that the empty edge zone had a particular effect with the elongated and irregular home ranges because ranges centered there would be expected to overlap the trap cells and be detected with non-zero probability. A deficit of detections attributable to such home ranges could lead to a lower SECR estimate of density. Estimates for the circular and square home ranges were unaffected because such ranges were too small to overlap the traps when they were centered in the edge zones; overlap would be expected for larger symmetrical ranges.

I tested two predictions that follow from this explanation. Eliminating the empty edge zone by distributing home ranges across the entire arena should effectively remove the bias with elongated or irregular home ranges, and increasing the size of symmetrical ranges should result in bias. Both predictions were confirmed in further simulations (Fig. 3g, i, j; Appendix S3).

Precision of SECR and TELEM with common benchmark

IWS used a different benchmark for each density estimator. For TELEM, true *D* was defined as the sum over simulated individuals of the known fraction of activity in the trapped cells *B* (in a sense, the realized population size of *B*), divided by the area of those cells. For SECR, true *D* was defined as the number of activity centers in

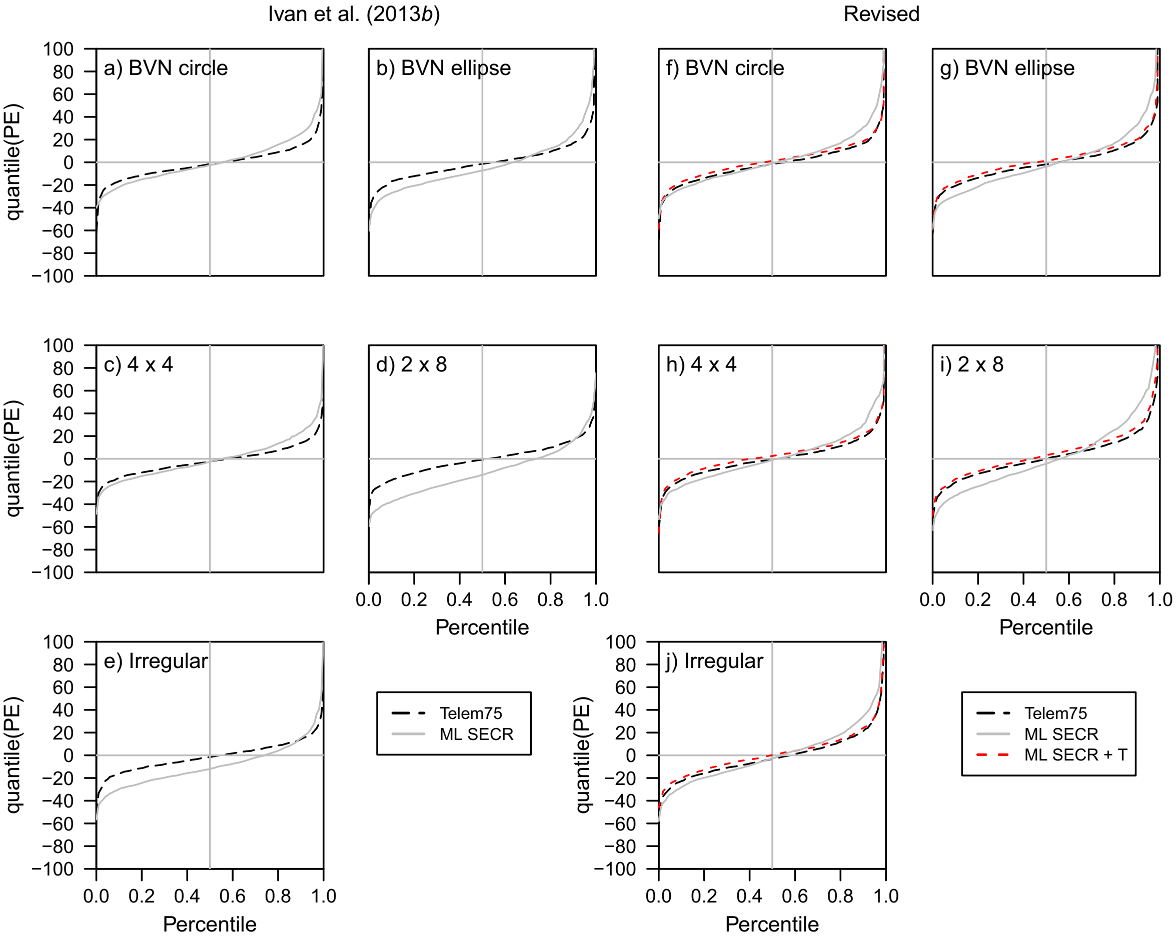

FIG. 3. Quantiles of percentage error (PE) for the telemetry-scaled non-spatial estimator (TELEM) and SECR estimators of population density applied to data simulated for various home-range shapes as in Ivan et al. (2013*b*). Panels a–e reproduce the corresponding panels of their figure. Panels f–j show the effect of correcting atefacts in the data simulation on the original SECR estimator, and a new estimator (ML SECR + T) for the realized population defined as for TELEM. Estimators whose curves intersect the crosshairs (quantile [PE] = 0 at 50th percentile) are median unbiased; precise estimators have a shallow slope at the 50th percentile.

the arena A divided by its area. The difference was presented by IWS as a matter of "fairness": each estimator was evaluated against the benchmark they considered most appropriate to it. TELEM is an estimate of the realized population density on a tightly circumscribed region, but SECR relates to the wider area from which animals are potentially caught.

In order to place the comparison on a more rigorous basis, I extended the concept of "realized population size" in SECR models to arbitrary small regions. This requires an estimate of the mean proportion of time spent inside the region by the individuals actually detected there, and a means of predicting the proportion for individuals present but not detected (Appendix S4). I repeated the simulations of IWS and computed the SECR estimate of the realized density on B, using the TELEM telemetry sample to estimate the mean proportion of activity falling in trapped cells. Quantile plots of the percentage error in these estimates with respect to the number of animal equivalents in the trapped cells (known from simulation) showed them to be almost indistinguishable from TELEM estimates (Fig. 3f–j). I note that under the conditions of these simulations, detected animals contributed almost all the realized density on B (detection probability is >90%) so capture–recapture contributes little to the estimates (Appendix S4).

Further Simulations with Aligned Elliptical Home Ranges

In the preceding simulations, activity ellipses were oriented independently at random. Further simulations considered alignment of the major axes of all individuals in a common direction relative to the detector array. For a square array, the options were "aligned" (ellipses parallel to one edge; Fig. 1b) and "oblique" (at 45 degrees to an edge; Fig. 1c); for a straight line of detectors the options were "parallel", "perpendicular," and "oblique". I report results only for highly elongated ranges (aspect ratio 4). Other conditions followed the initial simulations with random orientation as detailed in Appendix S2.

Alignment of highly elongated home ranges to a linear detector array generated bias in density estimates from mis-specified (circular) SECR models (Table 1a). Bias could be very positive or very negative depending on orientation, and coverage of confidence intervals (CI) was poor. The model is clearly useless in these circumstances. The circular model was also compromised when ellipses aligned with the rows or columns of a regular grid.

Anisotropic detection functions

Murphy et al. (2016; also B. Augustine, *personal communication*) allowed for range elongation by basing the SECR detection model on Euclidean distances computed in a space transformed to make home ranges more nearly circular. Transformation is straightforward when elliptical ranges are all oriented in the same direction and elongated to the same degree. The parameters for orientation and elongation may be estimated, along with the usual density and detection parameters, by maximizing the likelihood in the software described in Appendix S1.

In simulations, the method was effective at reducing bias due to aligned and elongated ranges in estimates from a 10 × 10 grid or hollow square, and CI coverage was improved (Table 1b). Estimation of the two anisotropy parameters had negligible effect on the precision of density estimates from the grid layout, but was costly with the more limited data from a hollow square (Table 1b).

Discussion

Robustness to non-circularity

Simulations provided evidence that SECR estimates of density are robust to elliptical elongation of home ranges

Table 1. Density estimates given elliptical home ranges (aspect ratio 4) modeled with (a) mis-specified (circular) detection function and (b) anisotropic detection function.

	Relative bias (%)			Relative SE (%)			Coverage of 95% CI (%)		
Orientation	Grid	Square	Line	Grid	Square	Line	Grid	Square	Line
(a) Mis-specified circular model									
Aligned	−8	−30	−75	8	16	16	79.8	36.8	0.0
Perpendicular	—	—	+179	—	—	17	—	—	0.0
Oblique	+2	+62	+94	8	18	16	94.4	30.6	2.2
Random	−1	+14	+17	8	17	18	94.0	80.0	76.4
(b) Anisotropic model									
Aligned	+1	+11	−82	8	26	28	95.6	89.0	1.0
Perpendicular	—	—	+150	—	—	44	—	—	25.5
Oblique	0	+17	+85	8	29	50	95.2	92.2	40.6
Random	−1	+8	−23	8	22	61	96.2	90.0	70.3

Notes: Simulated data from populations sampled with three detector geometries (10 × 10 grid, 36-detector square, 36-detector line) and varying rules for orientation. Dashes indicate infeasible scenarios. There were 500 replicates; perpendicular ellipses yielded estimates for only (a) 382 replicates and (b) 371 replicates, owing to a lack of spatial recaptures.

when sampling is not directionally biased. Estimates were also nearly unbiased with elliptical, rectangular, and irregular home ranges in the simulation scenarios of IWS when these were adjusted to remove idiosyncratic features. Conversely, artifactual bias could be generated with symmetrical (circular or square) home ranges in the scenarios of IWS by merely increasing their size.

These results support the assertion of Borchers and Efford (2008) that the SECR density estimator does not strictly require home ranges to be circular. There was no evidence to support the prediction of Efford (2004) that non-circularity would impair the precision of SECR density estimates. Robustness to non-circularity may be added to a list of other desirable SECR properties, including robustness to mis-specification of the detection function (Efford 2004), and qualified robustness to individual heterogeneity in home-range size (Efford and Mowat 2014) and transience (Royle et al. 2016).

However, simulations revealed that the SECR estimator may perform very poorly when non-circular home ranges are sampled with linear detector arrays, especially when the array aligns systematically with the axis of elongation. This is intuitively sensible: SECR relies on re-detections of individuals to estimate the spatial scale of detection σ and with a strictly linear array, $\hat{\sigma}$ only reflects movement along the array. A circular detection model based on $\hat{\sigma}$ will therefore predict more or fewer detected individuals depending on whether the major or minor axis of each home range is sampled preferentially (Murphy et al. 2016). Some positive bias remains even when elongated home ranges are oriented at random with respect to a linear array (Table 1). Estimates from elongated home ranges are also somewhat biased when detectors are arranged in a hollow square, despite this design sampling both east-west and north-south movements. The reason for these residual biases has not been determined.

Modeling noncircularity

An obvious potential solution to the residual issues with non-circular ranges is to model the non-circularity. The anisotropic model of Murphy et al. (2016) is effective when home ranges are oriented and elongated uniformly, and there is sufficient information from re-detections in two dimensions to estimate the corresponding parameters.

In the SECR models of Royle et al. (2013) and Sutherland et al. (2015), home ranges are molded by the landscape and can take a wide variety of shapes. However, their approach confounds home-range shape and size, and implies that animals centered in less-preferred (presumably resource-poor) habitats have smaller home ranges. This conflicts with both biological intuition and the evidence for a negative relationship between density and home range size (Efford et al. 2017), so further development would seem to be needed. A special case arises when movement strictly follows a linear or dendritic habitat feature such as a river system. Density is then expressed per unit length rather than per unit area, and distance is computed along the linear network without assuming circularity (Efford 2017).

Sensitivity to placement of detectors

The spatial artifacts discovered in the simulations of IWS emphasize a need for care in spatial sampling that carries over to field studies. It should not be surprising that a detector array will measure population density in its immediate vicinity and not elsewhere. For example, Gerber and Parmenter (2015) reanalysed data on known populations of desert rodents in fenced enclosures sampled with centrally placed trap arrays. Their inference that SECR estimates were biased rests on the assumption that the fence did not affect the distribution of rodents. It is possible that some species were more or less common near the fence, so that estimates from the centrally placed arrays did not reliably predict the entire population. The fence may also have aligned animal movements with respect to the trap arrays. Bias of the estimator in these conditions cannot be generalized to more typical scenarios.

Implications for study design

The preceding results can be restated as requirements for good spatial study design in SECR:

1) If home ranges are potentially elongated, then detector arrays should be two-dimensional to ensure that recaptures inform the spatial scale of detection in two dimensions. This is critical if ranges may share a common orientation due to alignment with landscape features. Alignment bias may be recognised and corrected by fitting anisotropic detection models when data are two-dimensional.
2) Placement of detectors in straight lines, or along linear features in two-dimensional habitat, risks severe bias that cannot be removed by the method of anisotropic detection functions. The effect varies with the degree of elongation and alignment. These may seldom be as extreme as simulated here, but as data from linear arrays provide no internal evidence on elongation their use will always be hazardous. The risk is potentially reduced by deploying multiple lines each with a random orientation.
3) Detectors sample the density of a population in their immediate vicinity. Selective placement of detectors in areas of above- or below-average density must be avoided if it is desired to infer density over a wider area. Areas of non-habitat where no animals are centered and no sampling occurs should be excluded from the model.

Realized density in a narrowly defined region

The method of Ivan et al. (2013*a*) narrows the region of interest for density to the immediate vicinity of the traps, from the broader region usually required as the region of integration in SECR (Borchers and Efford 2008: the "habitat mask" of Efford [2018] or the "state space" of Royle et al. [2014]). This is possible with both their non-spatial method and SECR if there is auxiliary information from telemetry of detected individuals (Appendix S4).

In the TELEM simulations of IWS, and the equivalent SECR simulations presented here, the resulting estimates are quite precise. However, the relative precision of narrow-region and wide-region estimates depends on the amount of telemetry data and the proportion of centrally located animals that are detected: the comparison may not always favor narrow-region estimates. By focusing on density in a narrowly defined region with high detection probability, the methods of Ivan et al. (2013*a*) and Appendix S4 may be better suited to answering some ecological questions, such as those requiring measurement of habitat covariates, especially if sampling is repeated at multiple sites.

ACKNOWLEDGMENTS

I thank Jake Ivan for cheerfully answering a number of questions, for access to SAS code, and for his thoughtful review. I am also grateful to Evan Cooch and three anonymous reviewers for their helpful comments.

LITERATURE CITED

Borchers, D. L., and M. G. Efford. 2008. Spatially explicit maximum likelihood methods for capture–recapture studies. Biometrics 64:377–385.

Boutin, S. 1984. Home range size and methods of estimating snowshoe hare densities. Acta Zoologica Fennica 171:275–278.

Efford, M. G. 2004. Density estimation in live-trapping studies. Oikos 106:598–610.

Efford, M. G. 2017. secrlinear: Spatially explicit capture–recapture for linear habitats. R package version 1.1.1. https://CRAN.R-project.org/package=secrlinear

Efford, M. G. 2018. secr: Spatially explicit capture–recapture models. R package version 3.1.7. https://CRAN.R-project.org/package=secr

Efford, M. G., and R. M. Fewster. 2013. Estimating population size by spatially explicit capture–recapture. Oikos 122:918–928.

Efford, M. G., and G. Mowat. 2014. Compensatory heterogeneity in spatially explicit capture–recapture data. Ecology 95: 1341–1348.

Efford, M. G., D. L. Borchers, and A. E. Byrom. 2009. Density estimation by spatially explicit capture–recapture: likelihood-based methods. Pages 255–269 *in* D. L. Thomson, E. G. Cooch, and M. J. Conroy, editors. Modeling demographic processes in marked populations. Springer, New York, New York, USA.

Efford, M. G., D. K. Dawson, Y. V. Jhala, and Q. Qureshi. 2017. Density-dependent home range size revealed by spatially explicit capture-recapture. Ecography 39:676–688.

Gerber, B. D., and R. R. Parmenter. 2015. Spatial capture–recapture model performance with known small-mammal densities. Ecological Applications 25:695–705.

Grant, T. J., and P. F. Doherty. 2007. Monitoring of the at-tailed horned lizard with methods incorporating detection probability. Journal of Wildlife Management 71:1050–1056.

Ivan, J. S., G. C. White, and T. M. Shenk. 2013*a*. Using auxiliary telemetry information to estimate animal density from capture–recapture data. Ecology 94:809–816.

Ivan, J. S., G. C. White, and T. M. Shenk. 2013*b*. Using simulation to compare methods for estimating density from capture–recapture data. Ecology 94:817–826.

Jennrich, R. I., and F. B. Turner. 1969. Measurement of non-circular home range. Journal of Theoretical Biology 22:227–237.

Murphy, S. M., J. J. Cox, B. C. Augustine, J. T. Hast, J. M. Guthrie, J. Wright, J. McDermott, S. C. Maehr, and J. H. Plaxico. 2016. Characterizing recolonization by a reintroduced bear population using genetic spatial capture–recapture. Journal of Wildlife Management 80:1390–1407.

R Core Team. 2018. R: A language and environment for statistical computing. R Foundation for Statistical Computing, Vienna, Austria. https://www.R-project.org

Royle, J. A., and K. V. Young. 2008. A hierarchical model for spatial capture–recapture data. Ecology 89:2281–2289.

Royle, J. A., R. B. Chandler, C. C. Sun, and A. K. Fuller. 2013. Integrating resource selection information with spatial capture–recapture. Methods in Ecology and Evolution 4:520–530.

Royle, J. A., R. B. Chandler, R. Sollmann, and B. Gardner. 2014. Spatial capture–recapture. Academic Press, Waltham, Massachusetts, USA.

Royle, J. A., A. K. Fuller, and C. Sutherland. 2016. Spatial capture–recapture models allowing Markovian transience or dispersal. Population Ecology 58:53–62.

Sutherland, C., A. K. Fuller, and J. A. Royle. 2015. Modelling non-Euclidean movement and landscape connectivity in highly structured ecological networks. Methods in Ecology and Evolution 6:169–177.

White, G. C., and T. M. Shenk. 2001. Population estimation with radio-marked animals. Pages 329–350 *in* J. J. Millspaugh and J. M. Marzluff, editors. Radio tracking and animal populations. Academic Press, San Diego, California, USA.

SUPPORTING INFORMATION

Additional supporting information may be found in the online version of this article at http://onlinelibrary.wiley.com/doi/10.1002/ecy.2580/suppinfo

DATA AVAILABILITY

Code is available from Zenodo: http://doi.org/10.5281/zenodo.1481187; http://doi.org/10.5281/zenodo.1481195.